nature geoscience

LETTERS

PUBLISHED ONLINE: 15 JUNE 2014 | DOI: 10.1038/NGEO2179

Deformation, warming and softening of Greenland's ice by refreezing meltwater

Robin E. Bell[1]*, Kirsteen Tinto[1], Indrani Das[1], Michael Wolovick[1], Winnie Chu[1], Timothy T. Creyts[1], Nicholas Frearson[1], Abdulhakim Abdi[1†] and John D. Paden[2]

Meltwater beneath the large ice sheets can influence ice flow by lubrication at the base or by softening when meltwater refreezes to form relatively warm ice[1–3]. Refreezing has produced large basal ice units in East Antarctica[4]. Bubble-free basal ice units also outcrop at the edge of the Greenland ice sheet[5], but the extent of refreezing and its influence on Greenland's ice flow dynamics are unknown. Here we demonstrate that refreezing of meltwater produces distinct basal ice units throughout northern Greenland with thicknesses of up to 1,100 m. We compare airborne gravity data with modelled gravity anomalies to show that these basal units are ice. Using radar data we determine the extent of the units, which significantly disrupt the overlying ice sheet stratigraphy. The units consist of refrozen basal water commonly surrounded by heavily deformed meteoric ice derived from snowfall. We map these units along the ice sheet margins where surface melt is the largest source of water, as well as in the interior where basal melting is the only source of water. Beneath Petermann Glacier, basal units coincide with the onset of fast flow and channels in the floating ice tongue. We suggest that refreezing of meltwater and the resulting deformation of the surrounding basal ice warms the Greenland ice sheet, modifying the temperature structure of the ice column and influencing ice flow and grounding line melting.

Over Lake Vostok[6] and along subglacial water networks in the Gamburtsev Mountains, Antarctica, ice refrozen to the base of the East Antarctic ice sheet has been mapped as reflections in ice-penetrating radar data[4,7]. In Greenland, similar features were first observed in the earliest ice-penetrating radar data recorded on black and white film during the 1970s (ref. 8). These reflections have previously been interpreted as energy returning from subglacial hills off to the side of the aircraft[9]. The basal ice beneath these reflectors often thickens along flow and deflects the overlying stratigraphy upwards. We have identified similar reflections and deflected stratigraphy in the northern half of Greenland using radar data from CReSIS and NASA's Operation IceBridge mission[10] (Fig. 1 and Supplementary Fig. 1). Our analysis of the new IceBridge gravity data[11] indicates that these features consist of ice (Supplementary Methods and Supplementary Fig. 2). The coherence of the units between the 10 km grid of IceBridge flight lines indicates that these reflections come from directly beneath the aircraft.

We have mapped the horizontal extent of these large features, which significantly deflect the ice sheet stratigraphy upwards, using the criteria that the Holocene layers[12] are deflected significantly (~200 m) upwards relative to the regional depth, the deflected internal layers are not conformable with the underlying bed topography, and a reflector is present within the unit. We identify basal units both along the ice sheet margin and within the interior. We examine the possibility that the basal units consist of refrozen meltwater and deformed meteoric ice.

Basal units up to 350 m thick occur in the ablation zone, between the mean snow line[13] and the ice margin. These marginal basal ice units are present in the Eqip catchment ~70 km north of Jakobshavn Isbræ, several outlet glaciers south of Rink Glacier and the Storstrømmen Branch of the Northeast Greenland Ice Stream (Fig. 1). Located in thin (<1,200 m) ice, these units are up to 20 km long and 10 km wide. Similar to features observed in the Gamburtsev Mountains[14] the marginal basal units tend to have bright upper reflections that extend from subglacial topographic lows. The marginal basal units are located within the region where, each summer, surface meltwater drains through moulins and crevasses to the base of the ice sheet. On the upslope edge of the marginal units, crevasses and moulins, inferred from surface imagery and radar scattering[15], provide pathways to the ice sheet bed for surface meltwater (Fig. 2 and Supplementary Fig. 3). Surface meltwater is probably the prime water source for the marginal basal units. Calculated hydrologic pathways[16,17] show that any basal meltwater formed in the interior of the ice sheet will be diverted away from the marginal basal units (Supplementary Fig. 4). Marginal units occur where the overlying ice drives the subglacial water up the steep bedrock topography and glaciohydraulic supercooling can contribute to the freeze-on[18].

In the interior, basal ice units are 200–1,100 m-thick packages of featureless ice that tend both to thicken downflow and to be bounded by upper layers of reflective ice. The nature of the upper reflection is variable and its character changes with different generations of radar data. In the Petermann and Northeast Greenland Ice Stream catchments, the well-defined interior basal units are generally aligned along flow (Fig. 3) and are located near calculated subglacial hydrologic pathways. In northern Greenland, water has flooded into deep boreholes[19] and radar data indicate meltwater is widespread at the base of the ice sheet[20] (Fig. 1b). Across many of the interior units, the ice surface flattens to almost half the regional slope. This change in surface slope suggests a reduction in the local basal shear stress due to the presence of water. As the interior features are found in the dry snow zone, no contribution from surface meltwater is anticipated. Basal meltwater in these subglacial water networks is the primary source of water that

[1]Lamont-Doherty Earth Observatory of Columbia University, Palisades, New York 10964, USA, [2]Center for the Remote Sensing of Ice Sheets, Kansas University, Lawrence, Kansas 66045, USA. †Present address: Department of Physical Geography and Ecosystem Science, Lund University, 210 00, Sweden. *e-mail: robinb@ldeo.columbia.edu

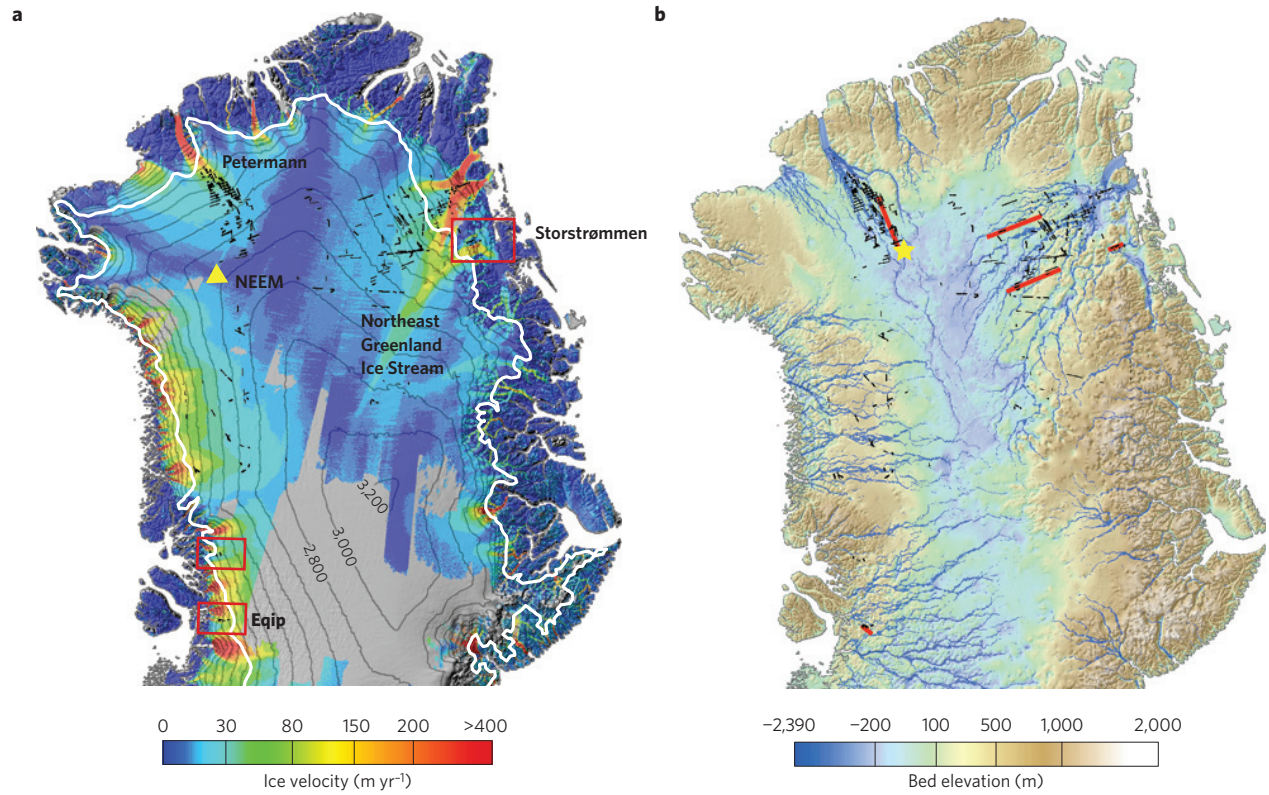

Figure 1 | Distribution of interior and marginal basal ice units in northern Greenland. a, Basal ice unit picks (black) shown over ice surface contours (200 m) and ice sheet velocity[25]. Red boxes outline marginal units. The mean snowline (1960–2012) is shown by the white line[13] and the location of the NEEM ice core by the yellow triangle. **b**, Basal ice picks over subglacial topography[30] overlain with the calculated subglacial hydrology network[16]. The yellow star indicates the bend in the Petermann subglacial valley. Red lines are profile locations (Figs 2 and 3). Often the basal units are identified by multiple radar profiles that constrain their spatial extent.

feeds the basal refreezing and the formation of the interior basal units (Fig. 1b).

The strata above these interior basal units are thinned and warped upwards (Fig. 3) into broad anticlines, similar to the stratigraphy over subglacial mountains[21], although the underlying bed topography is smooth. The strata overlying the interior basal units includes ice from the Holocene and Last Glacial Maximum as well as older ice, possibly from last interglacial (Eemian) (Supplementary Fig. 5). These strata were sampled by the NEEM core[22]. These strata, including the transparent Last Glacial Maximum ice and the underlying older layers, normally found close to the bottom of the ice sheet, have been transported towards to the ice surface, disrupting the normal stratigraphy of the ice column. The surrounding ice is also deformed. In front of these units, the lower half of the ice sheet is overturned into 5–10 km-wide recumbent folds with younger ice beneath older ice (Fig. 3b). Upstream of the basal units, the ice is deflected downwards into 10 km-wide synclines (Figs 3 and 4 and Supplementary Figs 5 and 6). Similar anticlines, synclines and recumbent folds are predicted in a model of freeze-on, dynamic basal slip contrasts and deformation triggered by basal water flow[14]. The rheologic contrast between the ice from the last glacial interval, characterized by small (1.5 mm) well-aligned crystals, and the underlying Eemian ice, characterized by larger (25 mm) crystal sizes with varying C axis orientations, may contribute to the deformation surrounding the interior basal units[22].

Without drilling into these units it is not yet possible to determine what fraction of the basal ice is refrozen and what is deformed meteoric ice. Nonetheless, low- and high-volume interpretations of the amount of refrozen ice are possible (Supplementary Figs 3 and 5). The high-volume estimate is that both the upper reflective interval and the underlying featureless ice are refrozen ice. The low-volume estimate is that only the 10–200 m-thick upper reflective layer is refrozen whereas the underlying ice is deformed meteoric ice. For each interpretation, the units are composed of refrozen water surrounded by highly deformed ice.

Together, the refreezing and deformation moves relatively warm ice (approximately −2.5 °C based on the temperature at the bottom of the NorthGRIP borehole)[23] 350–1,700 m upwards to the middle of the ice sheet, where the ambient temperature of the ice is 15–20 °C cooler. The advection of warm basal ice upwards during deformation changes the temperature structure of the ice column. The formation of basal units by freeze-on also influences the ice sheet temperature by releasing latent heat. Together these processes warm and soften the ice column.

The ice dynamic consequences of the refreezing and deformation are indicated by the interior basal ice units in the Petermann catchment (Fig. 4). The Petermann basal units are observed at a bend in the estimated subglacial water network along a prominent subglacial valley[24] (Fig. 1b). Twelve individual units are aligned along three flowlines, which extend from the edge of the subglacial valley to close to the grounding line. The onset of fast flow in the Petermann catchment[25] is a 18 km-wide tongue beginning 200 km inland from the grounding line and is in the region characterized by basal units (Fig. 4). The onset of fast flow is coincident with a basal unit. In the onset region, the ice moves 10–100% faster than the adjacent ice. As the basal unit widens and thickens, the fast flowing onset region also widens and the ice speeds up. The ice containing the basal units is not thicker than the adjacent ice. The onset of fast flow seems to

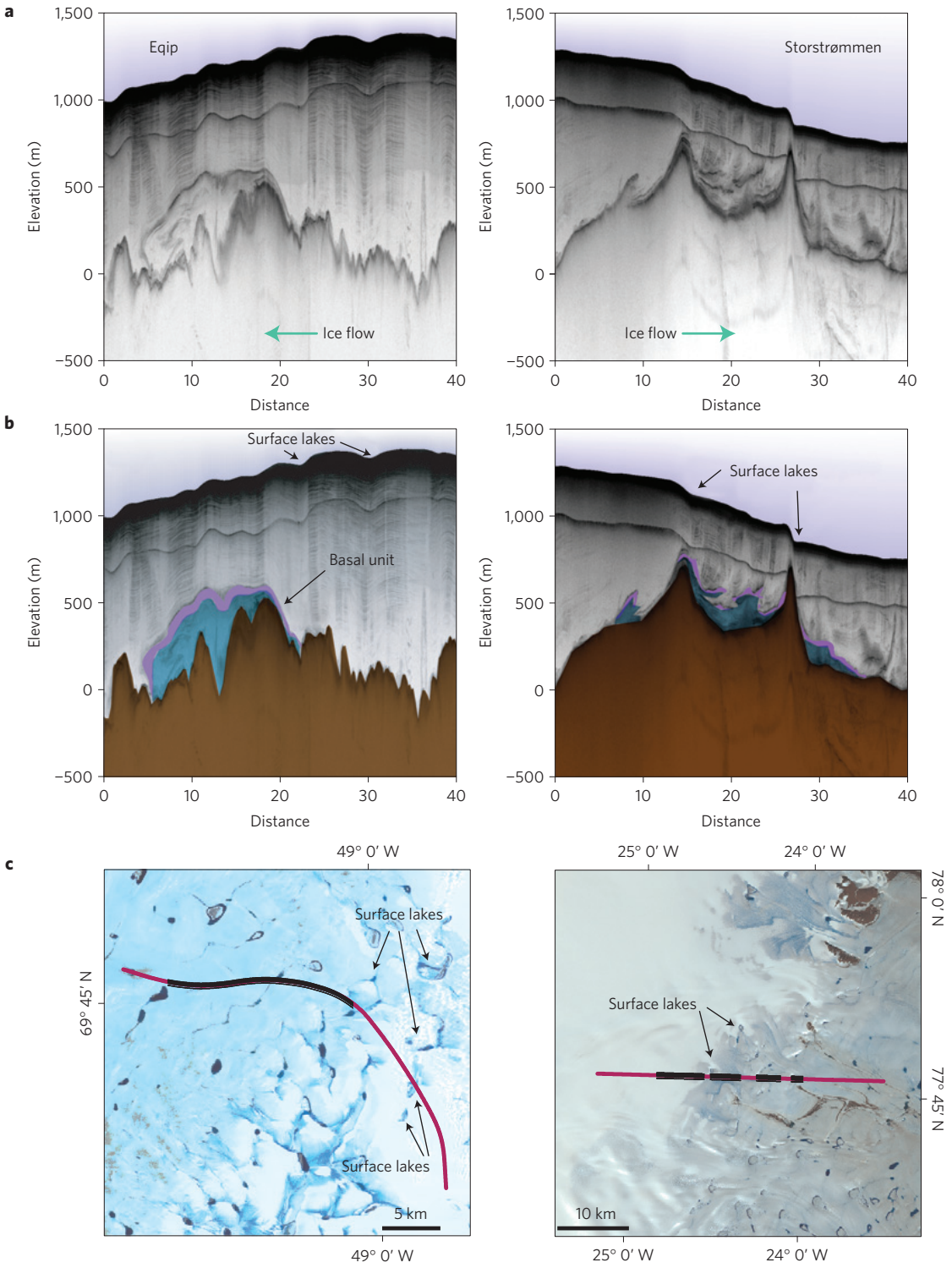

Figure 2 | Ice-penetrating radar data over marginal basal ice units and satellite imagery illustrating their presence in the ablation zone. Left column: Eqip (OIB Flight 20120421). Right column: Storstrømmen (OIB Flight 20120507). **a**, Ice-penetrating radar data. **b**, Radar interpretation: blue is basal unit and purple is bright upper reflection. **c**, Satellite imagery of ice surface and radar profile locations (red) with extent location of basal units (black). Profile locations are shown in Supplementary Fig. 4. Landsat imagery: left, 9 July 1999; right, 2 July 2001.

be localized along the edges of a prominent basal unit that forms along a hydrologic pathway. Warmer, softer ice within the basal unit, together with lubrication at the ice sheet base, contribute to the onset of fast flow.

The shallowest strata and the ice surface are also modified by the basal freeze-on and deformation. Over a large syncline in Petermann catchment, we observe a 20 m depression on the surface (Supplementary Fig. 6). The shallow strata over this 10 km-wide depression are thickened by up to 20%, indicating there is an increase in surface accumulation, probably from wind-drifted snow.

Localized melting of the Petermann ice tongue and the formation of a deep melt channel occurs in line with a prominent 140 km-long

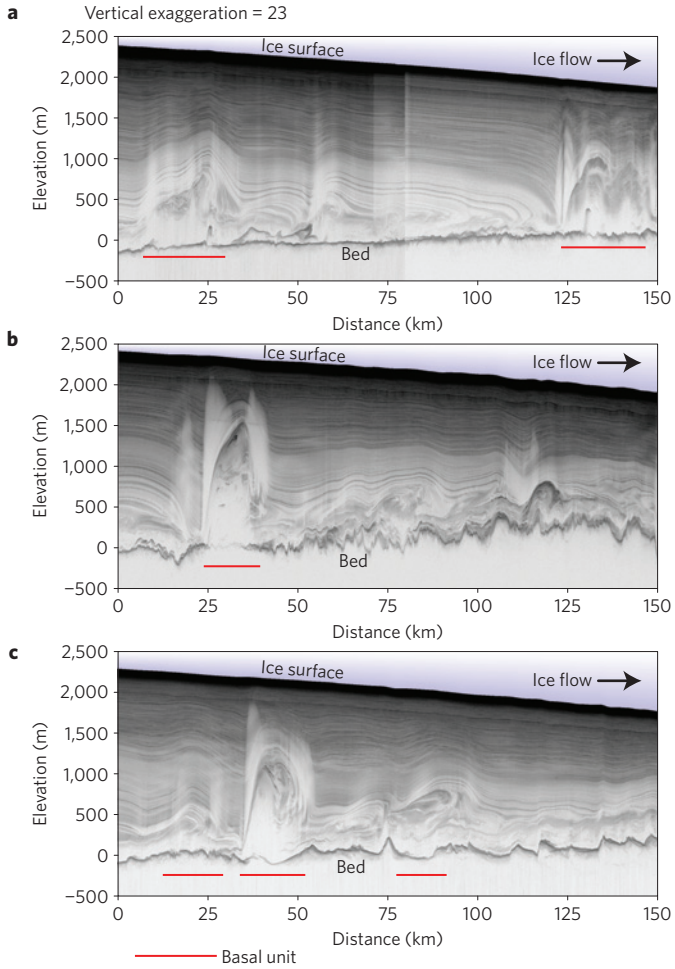

Figure 3 | Interior basal ice units imaged with ice-penetrating radar in northern Greenland. a, Petermann Ice Stream (OIB Flights 20120514 and 20110429). **b**, Northeast Ice Stream south (OIB Flight 201200507). **c**, Northeast Ice Stream north (OIB Flight 201200514). Locations of profiles are shown in Fig. 1. Red bars mark the horizontal extent of basal units. The modern 16-element IceBridge radar has other structures in the base of the ice sheet, including bright reflectors, folds and a fuzzy layer coincident with the Eemian ice sampled at NEEM (SM5).

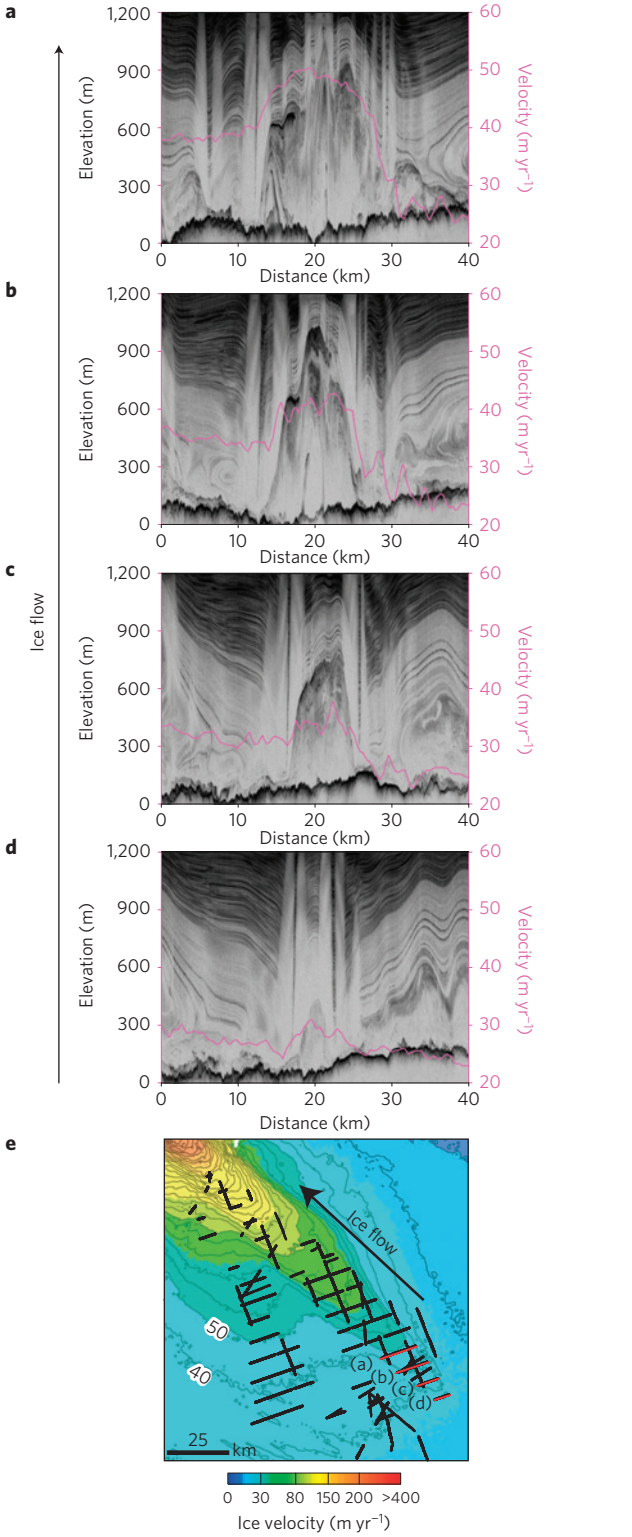

Figure 4 | Development of interior basal unit in the onset of fast flow in the Petermann catchment. a–d, Radar profiles perpendicular to ice flow with ice velocity overlain (magenta) over the basal unit. **e**, Close-up of the onset of fast flow. Basal ice units picks (black) overlain on surface velocity. The location of profiles **a–d** are shown in red (OIB flight 20110429).

basal unit that can be traced to within 40 km of the grounding line. This basal unit (2 km wide and 500 m high) is aligned with a similar sized melt channel where the ice sheet goes afloat (1 km wide and 400 m deep, Supplementary Fig. 7)[26]. At the grounding line, meltwater channels in floating ice can be localized where the warm, impurity-rich ice of the basal units is more easily melted or subglacial water focuses turbulent mixing of the ocean[27].

The close proximity of basal units to sources of subglacial water indicates refreezing is widespread and occurs in many environments beneath ice sheets. In well-surveyed areas, 10–13% of the base of the ice sheet and up to a third of the catchment width is modified by basal freeze-on. The interior units develop over relatively subdued topography with modest water flux from basal melt where conductive cooling probably dominates. The relatively steep bed topography and greater water flux from surface melt where the marginal units form suggests that supercooling plays a greater role in their formation. Both mechanisms of freeze-on will act in concert in varying proportions depending on the ice surface slope relative to bed slope, the ice thickness, ice velocity, the water pressure, the accumulation rate and the surface temperature. An impurity content analysis of the marginal units should reflect the relatively fresh surface melt, whereas the interior units probably reflect solute-rich basal melt.

Freeze-on of both surface and basal meltwater to the base of the Greenland ice sheet deforms the stratigraphy and modifies

the temperature structure and rheology of the ice. Other factors, including variable basal conditions[28], changing crystal fabric[29] and the contrasting rheology of glacial and interglacial ice[22] may contribute to the deformation. In the Petermann catchment, the routing of the water networks along a subglacial valley provides a fixed location for refreezing and deformation. The onset of fast flow in the Petermann catchment is localized along a large interior basal unit over a subglacial hydrologic pathway. The warming of the ice sheet by the basal unit refreezing and deformation, as well as basal sliding over the subglacial water, contribute to the onset of fast flow. The refreezing and deformation also moves ice normally found at the bottom of the ice sheet closer to the surface. Atop the broad anticlines over basal units, old ice from the last interglacial (possibly including Eemian strata) is found relatively close to the ice surface. Drilling these refrozen and deformed units will recover important climate records, provide insights into the amount of refreezing and advance our understanding of how the refreezing and deformation modifies ice sheet rheology. The presence of these large basal units resulting from refreezing and deformation indicates the influence of basal water reaches high into the ice sheet.

Methods

Gravity modelling over Petermann basal unit. Gravity models can be used to determine the density distribution that produces the observed gravity field. Here we use NASA IceBridge gravity data to demonstrate that the units defined by strong reflectors in the ice-penetrating radar have the same density as the surrounding ice. If the radar features were the result of off-nadir reflections from a nearby sub-glacial mountain then a positive gravity anomaly would be observed. Along a 55 km-long profile orthogonal to ice flow crossing the Petermann catchment the basal unit is at 30 km (Supplementary Fig. 2a). The observed gravity anomaly is shown above the radar profile. A simple gravity model assuming the basal unit at 30 km consists of rock with a density of 2.67 g cm^{-3} with a linear correction across the profile to account for the regional field would yield a gravity anomaly of 19 mGal centred over the basal unit (Supplementary Fig. 2b). No such gravity anomaly is centred over the basal units surveyed. The observed gravity field is closely matched by a model where the basal unit consists of ice (Supplementary Fig. 2c).

Radar profiles across interior basal units and age of strata. We dated the radar internal layers by comparison with a radar profile that passed through the NEEM ice core (Supplementary Fig. 5c). The NEEM ice core is 170 km away from our radar profile (Fig. 1). The NEEM ice core is located on one of the ice divides from which the Petermann and nearby glaciers originate. Similar to radar data from the NEEM site, the Petermann radar profile showed a set of three relatively undisturbed layers. The centre of these three layers is dated at NEEM to 46.85 kyr. The 84.8 kyr layer that seems undisturbed in the NEEM radar profiles is often deformed and uplifted as a result of basal refreezing in the Petermann catchment. The ice below this layer is also highly deformed. At 78.64° latitude, the 84.8 kyr layer is forced up into the ice sheet from ~2,100 m depth in the ice sheet to a depth of ~1,500 m. The ice below this layer is expected to be a mixture of highly deformed Eemian ice and refrozen meltwater. The temperature profile of an ice sheet generally increases with depth, with highest temperatures measured at the base. Thus, englacial uplift will warm the ice column by advecting warm basal ice higher into the column. This process will modify the temperature profile of the ice column along with latent heat released by freeze-on.

Analysis of accumulation over Petermann basal units. To derive the accumulation anomaly proxy, we traced six internal layers in the upper 40 m in the shallow ice radar. Then we differenced the depths of each layer from one another in all possible pairs. As the internal layers are each at different depths and we use all possible pair combinations, the depth difference between each pair is normalized by the difference in their average depths. The accumulation anomalies from all the pairs have similar ranges and are averaged to estimate an accumulation anomaly proxy (Supplementary Fig. 6a). This accumulation anomaly proxy indicates the spatial differences in surface accumulation influenced by the basal units.

Alignment of melt channels in ice tongue with Petermann basal units. The grounding line of the Petermann Glacier in Greenland terminates in a long fjord covered with an ice tongue. At the grounding line, the 1,000 m-thick floating ice tongue is modified by melting focused along three well-defined melt channels. These basal melt channels are 1–2 km wide and 200–400 m deep. The melting rate in the channels reaches 18 m yr^{-1}. The prominent central basal melt channel identified by Rignot and Steffen[26] is evident in the ice thickness map for the ice tongue shown on the map on the left of Supplementary Fig. 7. The basal units in the Petermann catchment are located in three discontinuous sequences aligned along the flow. One of the basal units can be traced for a distance of 140 km to within 40 km of the grounding line. Radar images of the two profiles closest to the grounding line are shown on the right of Supplementary Fig. 7. The basal unit is 2 km wide and 500 m thick. The coincidence of the basal unit with the central melt channel at the grounding line raises the possibility that the refrozen and deformed ice in the basal units plays a role in focusing or localizing the melting at the grounding line. The dotted line shows the possible extension of the basal unit towards the grounding line. The impurity content, crystal structure and temperature of the basal units may differ from the surrounding unmodified meteoric ice.

Received 1 November 2013; accepted 2 May 2014; published online 15 June 2014

References

1. Stearns, L. A., Smith, B. E. & Hamilton, G. S. Increased flow speed on a large East Antarctic outlet glacier caused by subglacial floods. *Nature Geosci.* **1,** 827–831 (2008).
2. Lliboutry, L. Local friction laws for glaciers: A critical review and new openings. *J. Glaciol.* **23,** 67–95 (1979).
3. Cuffey, K. M. & Paterson, W. S. B. *The Physics of Glaciers* (Academic, 2010).
4. Bell, R. E. *et al.* Widespread persistent thickening of the East Antarctic ice sheet by freezing from the base. *Science* **331,** 1592–1595 (2011).
5. Reeh, N., Oerter, H. & Thomsen, H. H. Comparison between Greenland ice-margin and ice-core oxygen-18 records. *Ann. Glaciol.* **35,** 136–144 (2002).
6. Bell, R. E. *et al.* Origin and fate of Lake Vostok water frozen to the base of the East Antarctic ice sheet. *Nature* **416,** 307–310 (2002).
7. Wolovick, M. J., Bell, R. E., Creyts, T. T. & Frearson, N. Identification and control of subglacial water networks under Dome A, Antarctica. *J. Geophys. Res.* **118,** 140–154 (2013).
8. Gudmandsen, P. Layer echoes in polar ice sheets. *J. Glaciol.* **15,** 96–101 (1975).
9. Legarsky, J., Wong, A., Akin, T. & Gogenini, S. P. Detection of hills from radar data in central-northern Greenland. *J. Glaciol.* **44,** 182–184 (1998).
10. Gogineni, P. in *CReSIS Radar Depth Sounder Data* (2012); http://data.cresis.ku.edu/
11. Cochran, J. R. & Bell, R. E. *IceBridge Sander AIRGrav L1B Geolocated Free Air Gravity Anomalies* (NASA DAAC at the National Snow and Ice Data Center, 2012).
12. Karlsson, N. B., Dahl-Jensen, D., Gogineni, S. P. & Paden, J. D. Tracing the depth of the Holocene ice in North Greenland from radio-echo sounding data. *Ann. Glaciol.* **54,** 44–50 (2013).
13. Van Angelen, J. H. *et al.* Sensitivity of Greenland ice sheet surface mass balance to surface albedo parameterization: a study with a regional climate model. *The Cryosphere* **6,** 1175–1186 (2012).
14. Wolovick, M., Bell, R. E., Roger Buck, W. & Creyts, T. T. *Controls on the Geometry of Accretion Reflectors abstr. C33E-03* (AGU Fall meeting, 2012).
15. Catania, G. A., Neumann, T. A. & Price, S. F. Characterizing englacial drainage in the ablation zone of the Greenland ice sheet. *J. Glaciol.* **54,** 567–578 (2008).
16. Flowers, G. E. & Clarke, G. K. C. Surface and bed topography of Trapridge Glacier, Yukon Territory, Canada: digital elevation models and derived hydraulic geometry. *J. Glaciol.* **45,** 165–174 (1999).
17. Shreve, R. L. Movement of water in glaciers. *J. Glaciol.* **11,** 205–214 (1972).
18. Creyts, T. T. & Clarke, G. K. Hydraulics of subglacial supercooling: Theory and simulations for clear water flows. *J. Geophys. Res.* **115,** F03021 (2010).
19. Andersen, K. K. *et al.* High-resolution record of Northern Hemisphere climate extending into the last interglacial period. *Nature* **431,** 147–151 (2004).
20. Oswald, G. & Gogineni, S. Recovery of subglacial water extent from Greenland radar survey data. *J. Glaciol.* **54,** 94–106 (2008).
21. Hindmarsh, R. C., Leysinger Vieli, G. J., Raymond, C. & Gudmundsson, G. H. Draping or overriding: The effect of horizontal stress gradients on internal layer architecture in ice sheets. *J. Geophys. Res.* **111,** F02018 (2006).
22. Dahl-Jensen, D. *et al.* Eemian interglacial reconstructed from a Greenland folded ice core. *Nature* **493,** 489–494 (2013).
23. Dahl-Jensen, D., Niels, G., Prasad Gogineni, S. & Miller, H. Basal melt at NorthGRIP modeled from borehole, ice-core and radio-echo sounder observations. *Ann. Glaciol.* **37,** 207–212 (2003).
24. Bamber, J. L., Siegert, M. J., Griggs, J. A., Marshall, S. J. & Spada, G. Paleofluvial mega-canyon beneath the Central Greenland ice sheet. *Science* **341,** 997–999 (2013).
25. Joughin, I., Smith, B., Howat, I. & Scambos, T. *MEaSUREs Greenland Ice Velocity Map from InSAR Data* (National Snow and Ice Data Center, 2010).
26. Rignot, E. & Steffen, K. Channelized bottom melting and stability of floating ice shelves. *Geophys. Res. Lett.* **35,** L02503 (2008).
27. Le Brocq, A. M. *et al.* Evidence from ice shelves for channelized meltwater flow beneath the Antarctic ice sheet. *Nature Geosci.* **6,** 945–948 (2013).

28. Joughin, I., Fahnestock, M., MacAyeal, D., Bamber, J. L. & Gogineni, P. Observation and analysis of ice flow in the largest Greenland ice stream. *J. Geophys. Res.* **106,** 34021–34034 (2001).
29. Horgan, H. J. *et al.* Complex fabric development revealed by englacial seismic reflectivity: Jakobshavn Isbræ, Greenland. *Geophys. Res. Lett.* **35,** L10501 (2008).
30. Bamber, J. L. *et al.* A new bed elevation dataset for Greenland. *The Cryosphere* **7,** 499–510 (2013).

Acknowledgements

The authors acknowledge support from NASA and NSF for this manuscript. The Operation IceBridge mission provided critical data for this analysis. The radar data from the CReSIS radar systems and the Sander Geophysics Ltd. AirGrav gravity data were central to this work. L. Altman, B. Bell and S. Starke provided support in analysis of the data and production of the figures. R. Buck provided feedback that improved the paper substantially. LDEO contribution number 7800.

Author contributions

R.E.B. designed the experiment as part of the NASA Icebridge Science Team. K.T. collected and analysed gravity data. I.D. conducted analysis of shallow and deep ice radar. M.W. conducted analysis of deep ice radar. W.C. conducted analysis of deep ice radar and the water routing calculation. T.T.C. contributed to the water routing calculation. N.F. conducted analysis of deep ice radar. A.A. conducted analysis of deep ice radar. J.D.P. collected and reduced radar data. All authors participated in the interpretation and writing of the paper.

Additional information

Supplementary information is available in the online version of the paper. Reprints and permissions information is available online at www.nature.com/reprints. Correspondence and requests for materials should be addressed to R.E.B.

Competing financial interests

The authors declare no competing financial interests.